Regional differences in radiosensitivity across the rat cervical spinal cord

Bijl, HP; van Luijk, P; Coppes, RP; Schippers, JM; Konings, AWT; van Der Kogel, AJ

Published in:
International Journal of Radiation Oncology Biology Physics

DOI:
10.1016/j.ijrobp.2004.10.018

Publication date:
2005

Int. J. Radiation Oncology Biol. Phys., Vol. 61, No. 2, pp. 543–551, 2005

0360-3016/05/$–see front matter

doi:10.1016/j.ijrobp.2004.10.018

BIOLOGY CONTRIBUTION

REGIONAL DIFFERENCES IN RADIOSENSITIVITY ACROSS THE RAT CERVICAL SPINAL CORD

HENDRIK P. BIJL, M.D.,* PETER VAN LUIJK, PH.D.,*‡ ROB P. COPPES, PH.D.,*†
JACOBUS M. SCHIPPERS, PH.D.,‡ ANTONIUS W. T. KONINGS, PH.D.,† AND
ALBERT J. VAN DER KOGEL, PH.D.§

*Department of Radiation Oncology, University Hospital Groningen, Groningen, The Netherlands; †Department of Radiation and Stress Cell Biology, University of Groningen, Groningen, The Netherlands; ‡Kernfysisch Versneller Instituut, Groningen, The Netherlands; §Department of Radiation Oncology, University Medical Center Nijmegen, Nijmegen, The Netherlands

Purpose: To study regional differences in radiosensitivity within the rat cervical spinal cord.
Methods and Materials: Three types of inhomogeneous dose distributions were applied to compare the radiosensitivity of the lateral and central parts of the rat cervical spinal cord. The left lateral half of the spinal cord was irradiated with two grazing proton beams, each with a different penumbra (20–80% isodoses): lateral wide (penumbra = 1.1 mm) and lateral tight (penumbra = 0.8 mm). In the third experiment, the midline of the cord was irradiated with a narrow proton beam with a penumbra of 0.8 mm. The irradiated spinal cord length (C1–T2) was 20 mm in all experiments. The animals were irradiated with variable single doses of unmodulated protons (150 MeV) with the shoot-through method, whereby the plateau of the depth–dose profile is used rather than the Bragg peak. The endpoint for estimating isoeffective dose (ED_{50}) values was paralysis of fore and/or hind limbs within 210 days after irradiation. Histology of the spinal cords was performed to assess the radiation-induced tissue damage.
Results: High-precision proton irradiation of the lateral or the central part of the spinal cord resulted in a shift of dose–response curves to higher dose values compared with the homogeneously irradiated cervical cord to the same 20-mm length. The ED_{50} values were 28.9 Gy and 33.4 Gy for the lateral wide and lateral tight irradiations, respectively, and as high as 71.9 Gy for the central beam experiment, compared with 20.4 Gy for the homogeneously irradiated 20-mm length of cervical cord. Histologic analysis of the spinal cords showed that the paralysis was due to white matter necrosis. The radiosensitivity was inhomogeneously distributed across the spinal cord, with a much more radioresistant central white matter (ED_{50} = 71.9 Gy) compared with lateral white matter (ED_{50} values = 28.9 Gy and 33.4 Gy). The gray matter did not show any noticeable lesions, such as necrosis or hemorrhage, up to 80 Gy. All lesions induced were restricted to white matter structures.
Conclusions: The observed large regional differences in radiosensitivity within the rat cervical spinal cord indicate that the lateral white matter is more radiosensitive than the central part of the white matter. The gray matter is highly resistant to radiation: no lesions observable by light microscopy were induced, even after a single dose as high as 80 Gy.

Dose–volume effects, Protons, Radiosensitivity, Spinal cord, White matter necrosis.

INTRODUCTION

In radiation oncology it is a major goal to irradiate the tumor with the highest possible dose with minimal morbidity of the normal tissue. Therefore, it is of great importance to know the adverse effects of inhomogeneous dose distributions on normal tissues and to be able to estimate normal tissue complication probabilities.

The total dose to the planning target volume is limited by the tolerance of surrounding healthy tissues. When a tumor is located near a critical organ, as often occurs with the spinal cord, the dose is likely to be inhomogeneously distributed across the cord. Although this situation is common in clinical practice, the influence of this inhomogeneous dose distribution on the tolerance of the spinal cord is not known. For homogeneously irradiated rat spinal cord with lengths <2 cm, it is known that the isoeffective dose (ED_{50}) for white matter necrosis decreases with increasing irradi-

Reprint requests to: Hendrik P. Bijl, M.D., Department of Radiation Oncology, University Hospital Groningen, Hanzeplein 1, Groningen 9700 RB, The Netherlands. Tel: (+31) 50-3613674; Fax: (+31) 50-3611692; E-mail: h.p.bijl@rt.azg.nl

Dr. Schippers's present address is the Paul Scherrer Institut, Villigen, Switzerland.

This study is a part of the Proton Therapy Project Groningen, financed (Centrale Beleiosruimte RUG [CBR]) by the University of Groningen in The Netherlands.

Acknowledgments—The excellent technical assistance of Harrie Kiewiet, Hette Faber, Femmy Cotteleer, Martha Ritsema, Wenny Peeters, and Annet Verleg is gratefully acknowledged.

Received Apr 9, 2004, and in revised form Oct 11, 2004. Accepted for publication Oct 13, 2004.

ated volume (1–3). In a recently published study (4) addressing inhomogeneous dose distributions over the longitudinal axis of the cord, we observed an unexpectedly large decrease of the ED_{50} for white matter necrosis for a 4-mm cord length when single doses as low as 4 Gy (bath doses) were applied to the regions adjacent to the 4-mm region. Histology of the spinal cord from paralyzed rats showed white matter necrosis predominantly in the lateral parts of the cord, without morphologic changes in the gray matter.

The pathogenesis of radiation-induced white matter necrosis is still not clear. Classically, the development of white matter necrosis has been considered a manifestation of a reduced number of surviving clonogens of either vascular or parenchymal target populations (5). Morris *et al.* (6) showed in boron neutron capture therapy experiments that endothelial cells were the most likely critical target population. There are several observations that, after irradiation, the oligodendrocyte progenitor cell (OPC)–depleted areas were repopulated by OPCs from adjacent unirradiated regions (7–9).

In the present study, we investigated the dose–response relationships for different regions across the rat cervical spinal cord. We selectively irradiated the left lateral half and a longitudinal slice along the midline of the spinal cord with a high-precision proton beam (150 MeV unmodulated protons), with a wide range of doses in gray and white matter. The obtained dose–response relationships are compared with a homogeneously irradiated 20-mm length of cervical cord (1). These experiments have benefited from the dose–distribution advantages of protons over the use of X-rays (mega- or kilovoltage). For protons, the penumbra at a 3-cm depth is as steep as could be achieved with orthovoltage X-rays, but contrary to orthovoltage X-rays, the depth–dose profile is more or less constant. This allows a very precise knowledge of the dose distribution in an absolute sense. The results of the experiments indicate that the higher radiosensitivity of the white matter compared with gray matter is not solely attributable to blood vessel damage and that a large difference exists between the sensitivity of central compared with more lateral regions of the white matter.

METHODS AND MATERIALS

Animals

Male Wistar rats weighing 200–250 g were used. After irradiation, the animals were housed 2 per cage and provided with food and water *ad libitum*. All experiments were carried out in agreement with The Netherlands Experiments on Animals Act (1977) and The European Convention for the Protection of Vertebrates Used for Experimental Purpose (Strasbourg, 18.III.1986).

Experimental setup

Six rats were anesthetized (2.5% isoflurane at 0.75 O_2 L/min for 10 min) and were placed vertically at equal distances in a Perspex frame with the head fixed. The distance between the spinal cords was 5 cm. The diameter (left–right) of the cervical spinal cord is approximately 3.5 mm. The spinal cord had to be positioned very accurately at the 50% dose level in the penumbra. To achieve the correct position, the frame was placed on a slider that could be moved with a remote-controlled stepping motor (160 steps per millimeter). After position verification with X-rays, the position of the frame in the beam could be adjusted. The X-ray tube was inserted in the system by remote control. Radiographs were registered with a digital fluoroscopic system (10). A charge coupled device (CCD) camera monitored a scintillating screen that detected the X-rays traversing the rat. One radiograph approximately deposited a dose of 3 mGy in the rat. The number of radiographs varied from one to three per rat.

The position of the 50% isodose line was determined from a picture of the 20 × 20-mm proton field. Next, a copper needle was placed at the isocenter and moved toward the position of the penumbra in the 20 × 20-mm proton field. This position was verified by making a proton image of this field. Then a radiograph was made of the needle with the X-ray imager. This image was laid over the image of the rat for determining where the spinal cord should be positioned. After setting up the frame with the rats, a radiograph was made in which the spinal cord was near the center of the 20 × 20-mm field. In this image both edges of the spinal cord were marked by hand. From these positions the location of the center of the cord and the distance between the center and the left edge were calculated. Then the rat was moved over the calculated distance, and a verification radiograph was made.

Comparison of the pre- and postirradiation images yielded an average displacement (systematic error) of only 0.008 mm, with a standard deviation (interanimal variation) of 0.08 mm. The maximum deviation found was 0.12 mm (10).

Grazing beam experiments. In this experiment, we applied a 20 × 20-mm field by using a 45-mm-thick brass collimator. In the first experiment (lateral wide), the edge of the field-defining collimator was centered on the axis of the proton beam. The spinal cord was positioned 15 cm downstream from the field-defining collimator. At this location and depth the penumbra of the proton field was 1.1 mm (Fig. 1a). For more details, we refer to the article of Van Luijk *et al.* (10). In the second experiment (lateral tight), the 45-mm-thick brass collimator was also positioned 15 cm in front of the spinal cord, but a second collimator was placed 7 cm in front of the spinal cord. The edge of this 45-mm-thick brass half-collimator was positioned on the axis of the proton beam. The penumbra of the proton beam at the isocenter was 0.8 mm (Fig. 1b). The cervical spinal cord was irradiated over a length of 20 mm (C1–T2) in both grazing beam experiments.

Central beam experiment. In this experiment, we applied a second 45-mm-thick brass slit collimator downstream of the first collimator (Fig. 1c). This slit collimator of 2 × 20 mm was centered on the proton beam 7 cm in front of the spinal cord. The slit was moved in and out by remote control to take X-ray photographs with a sufficiently large field of view. The verification protocol of the maximum absolute dose in the dose distribution (D_{max}) at the center of the spinal cord was the same as in the grazing beam experiments, and the width of the penumbra was 0.8 mm.

Irradiation protocol

In the three experiments, the cervical spinal cord was irradiated with variable single doses of unmodulated 150-MeV proton beams (Table 1) from the AGOR (Accelerateur Groningen ORsay) cyclotron of the Kernfysisch Versneller Instituut in Groningen, The Netherlands. For protons, the lateral penumbra at a 3-cm depth is as steep as could be achieved with orthovoltage X-rays. The 20–80% isodoses penumbra for protons

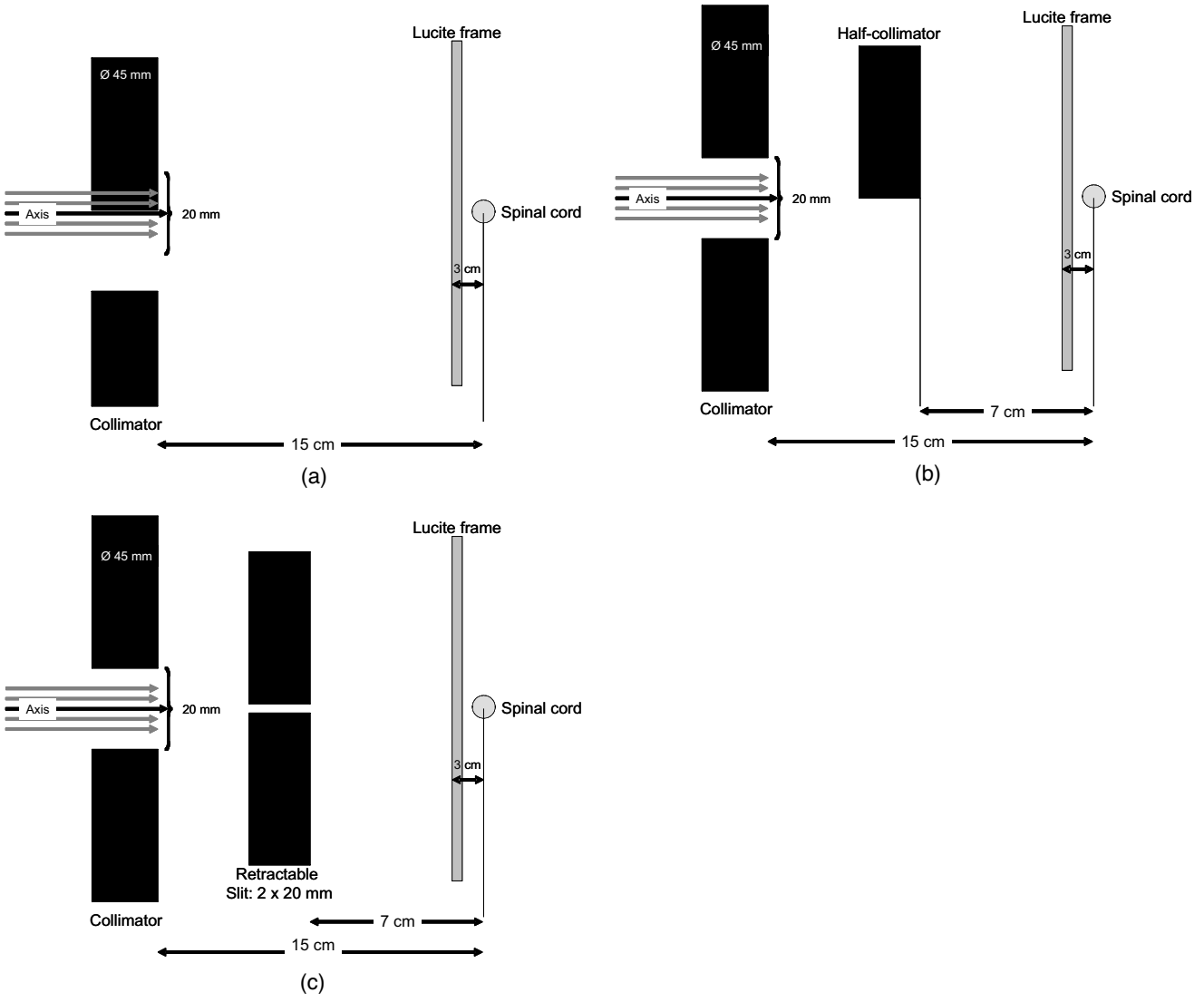

Fig. 1. Schematic view of the setup for the three experiments: lateral wide (a), lateral tight (b), and central beam (c).

and X-rays are comparable, but the 10–90% isodoses penumbra is smaller for protons. Contrary to orthovoltage X-rays, the depth–dose profile of protons is more or less constant. This allows a very precise knowledge of the dose distribution in an absolute sense. To achieve a constant depth–dose profile with othovoltage X-rays, the spinal cord has to be irradiated from both the ventral and dorsal side of the rat. The extra irradiation leads to less accuracy in the positioning of the spinal cord and to a less effective penumbra.

Dosimetry

The dose profiles were measured in two dimensions with the CCD/scintillator system developed by Boon *et al.* (11), which has a spatial resolution of σ = 0.22 mm (12). These dose profiles were calibrated before the first irradiation with a 0.6-cm^3 cylindrical ion chamber (PTW-30001 Farmer chamber; PTW, Freiburg, Germany) at the position of the spinal cord in a Ø 70-mm field. The output factors of the 20 × 20-mm and 2 × 20-mm fields with respect to the Ø 70-mm field were found by comparing screen measurements, taken at an equal number of monitor units (10). The reported dose values are the 100% values (Fig. 2).

Dose–area histogram

Animals were anesthetized (1.3% isoflurane; 1:1 [vol/vol] N_2O/O_2 mixture) and positioned in a magnetic resonance (MR) spectrometer. Forty contiguous transverse MR images were acquired in a standard multislice spin-echo experiment. In a transversal cross-section at level C4 of the MR imaging scan, a contour of the spinal cord was defined. With this contour and the measured dose distributions, a cumulative dose–area histogram could be obtained. For more details, we refer to the article by Van Luijk *et al.* (10).

Endpoints

The animals were checked for the development of paralysis of fore and hind limbs regularly, at least twice weekly. The cutoff time to establish the endpoint for paralysis due to white matter necrosis was set at 7 months (13). This cutoff point was chosen because the incidence of paralysis due to white matter necrosis

Table 1. Overview of the experiments

Experiment	Dose (Gy) per group (No. of responders/ irradiated rats)	Latent period (days) ± SEM	ED_{50} (Gy)	95% CI
Grazing beam (lateral wide)	20 (0/4)		28.9	
	25 (0/4)			
	30 (3/4)	160 ± 20.8		
	35 (4/4)	134.5 ± 9.4		
	40 (4/4)	126.5 ± 3.5		
Grazing beam (lateral tight)	24 (0/3)		33.4	31.9–36.2
	26 (0/3)			
	28 (0/6)			
	30 (1/6)	146		
	32 (0/6)			
	34 (2/3)	139 ± 18		
	36 (4/4)	141.3 ± 5.2		
Central beam	20 (0/3)		71.9	65.5–87.9
	24 (0/6)			
	28 (0/6)			
	30 (0/4)			
	32 (0/6)			
	36 (0/3)			
	40 (0/6)			
	50 (0/6)			
	60 (1/6)	98		
	70 (1/6)	70		
	80 (4/4)	62.5 ± 2.8		
20-mm single field (1)	18 (0/6)		20.4	
	20 (1/6)	169		
	22 (6/6)	170 ± 4.8		
	24 (6/6)	165.8 ± 5.1		

Abbreviations: CI = confidence interval; SEM = standard error of the mean.

occurs within a latent period of 5–6 months. An extra month was added to the follow-up period to account for the very few relatively late responders (13). The nonresponders were kept in follow-up for a period of up to 20 months to monitor a possibly developing second wave of paralysis. A second wave of paralysis was previously described by Hopewell *et al.* (2) and Van der Kogel *et al.* (14) after irradiation of short lengths of the rat spinal cord and was related to late vascular damage.

After single doses of 20–40 Gy, white matter necrosis is observed in the lateral and ventrolateral parts of the white matter. The damage at these anatomic sites is functionally expressed as paralysis of the fore limbs. After very high single doses (>40 Gy), the necrosis is more widely distributed within the white matter, including the ventral and dorsal tracts. This extensive damage is reflected in the paralysis of fore and hind limbs. Animals were scored as responders when they showed paralysis of the fore and/or hind limbs. The time from irradiation to the time of paralysis is referred to as the latent period. When paralysis had developed, the rat was killed and the spinal column removed and fixated in formalin 4% for at least 24 hours. After fixation, the spinal column was decalcified in a mixture of sodium formiat 8% and formic acid 40% for a period of 7 days, after which the spinal cord was processed with a standard paraffin-embedding method for routine hematoxylin-eosin staining. The blocked spinal cord tissue was sectioned at 4 μm and mounted on microscopic slides.

Two rats died without neurologic symptoms and were recorded as intercurrent deaths ($n = 2$). Both rat deaths were not related to the experiment. Only animals with paralysis were recorded as responders.

Statistical analysis

The dose–response curves were constructed by probit analysis. SPSS 9.0 (SPSS, Chicago, IL) was used for statistical analysis.

RESULTS

Grazing beam experiment

The dose–response curves for the lateral wide and tight experiments shifted to higher doses compared with the dose–response curve for the 20-mm full field (Fig. 3). The lateral tight irradiation, with a 0.3-mm smaller penumbra, resulted in a 4.5-Gy higher ED_{50} than the lateral wide irradiation. Both the lateral wide and tight experiments showed significantly higher ED_{50} than the 20-mm full field (Table 1).

The 100% isodose in both experiments was located at the lateral part of the white matter. All responders showed unilateral paralysis of the left fore limb after doses ≥30 Gy. The 100% responders in the lateral wide experiment were observed after 35 Gy and in the tight group after 36 Gy. In contrast, the 20-mm full field showed first response after a single dose of only 20 Gy, with 100% response after ≥22 Gy.

The latent periods for responders are shown in Fig. 4. The mean latent periods for the lateral wide and lateral tight experiments varied from 126.5 to 160 days and 141.3 to 146 days, respectively (Table 1).

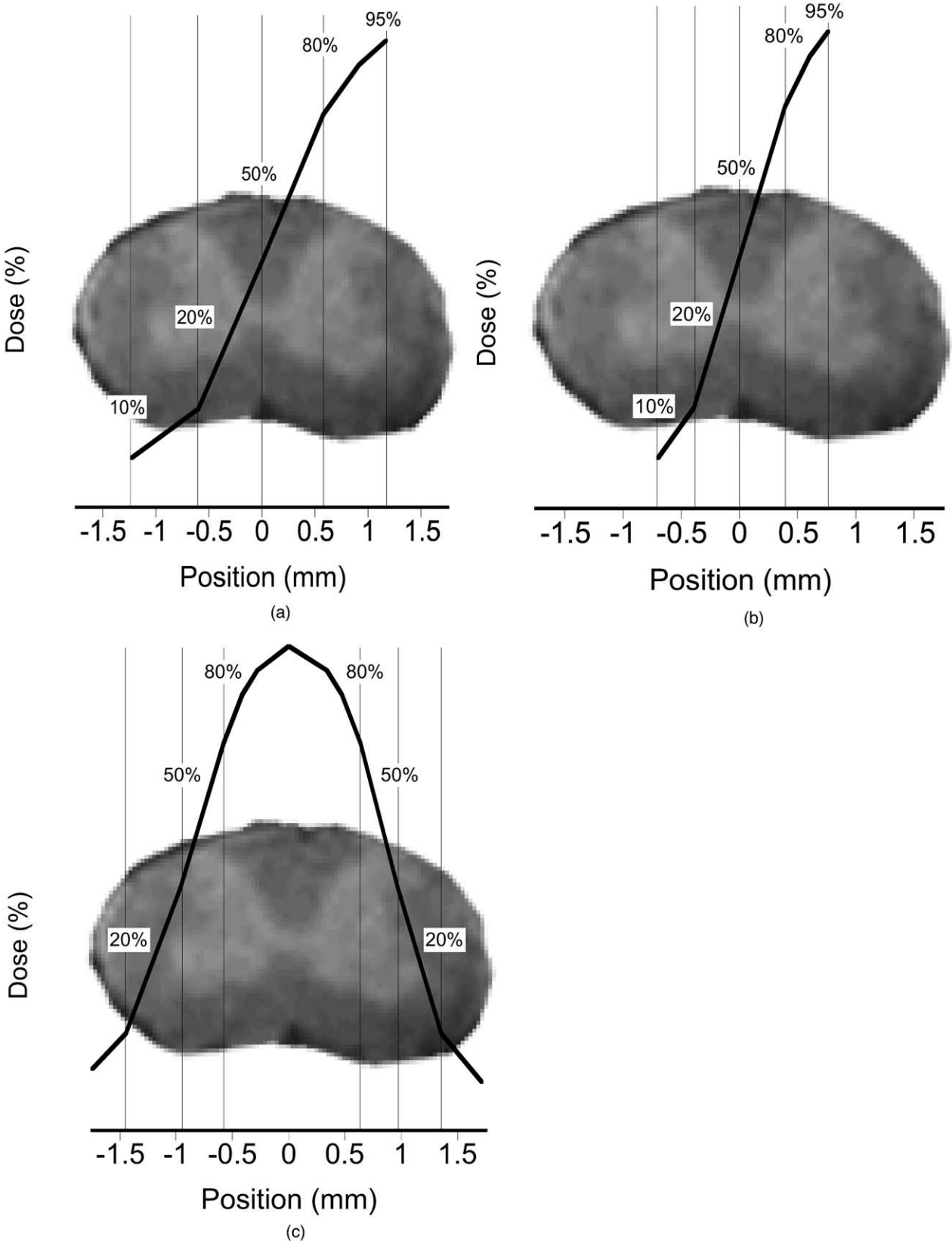

Fig. 2. The dose distributions for the grazing and central beam experiments are projected on a transversal MR image of the cervical spinal cord. (a) Lateral wide, (b) lateral tight, (c) central beam.

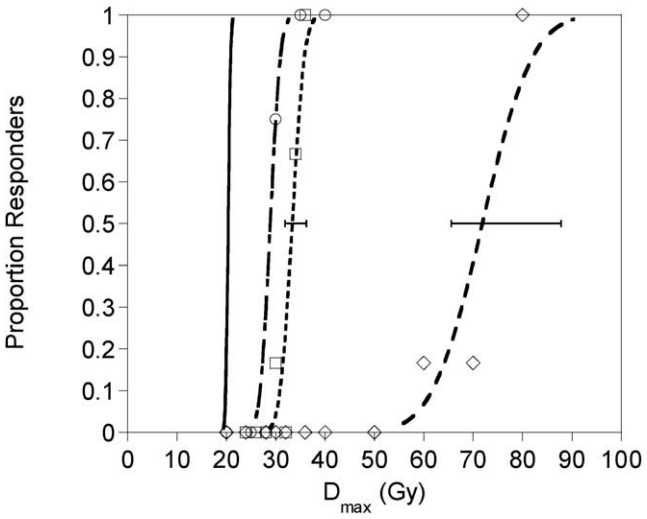

Fig. 3. Dose–response curves for paralysis after lateral wide (circles), lateral tight (squares), and central beam (diamonds) irradiation compared with the 20-mm full-width irradiation (1). Error bars: 95% confidence interval.

Histology of the spinal cord from paralyzed rats showed areas of white matter necrosis in the lateral part of the left irradiated half of the spinal cord. No histologic changes were observed in the right half and in the middle part consisting of gray and white matter (Fig. 5a). The peripheral nerve roots were undamaged and without morphologic changes. Rats with a follow-up period of up to 20 months never showed neurologic deficits. No changes were seen in the white or gray matter of nonresponders.

Central beam experiment

In contrast to the grazing beam experiments, an unexpectedly large shift to higher doses of the dose–response curve was observed (Fig. 3). The ED_{50} value for the central beam increased by a factor of 3.5 compared with the 20-mm full-field value (from 20.4 to 71.9 Gy) (Table 1). The 95% confidence intervals for the central beam and the grazing beam experiments showed no overlap (Table 1).

The responders showed paralysis of the fore limbs and were only seen after doses ≥60 Gy. In contrast, the threshold dose for white matter necrosis in a 20-mm full-field irradiation was 20 Gy (1).

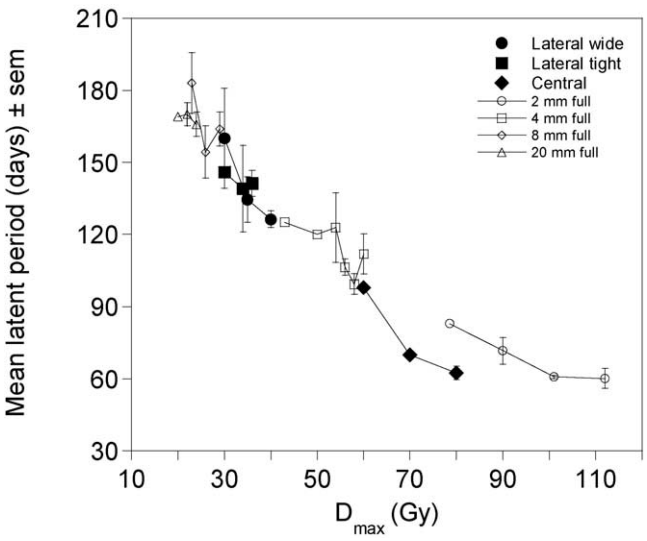

Fig. 4. Latent periods for the lateral wide (black circles), lateral tight (black squares), and central beam (black diamonds) irradiations compared with the latent periods for the homogeneous single-field irradiations (1). Error bars: standard error of mean.

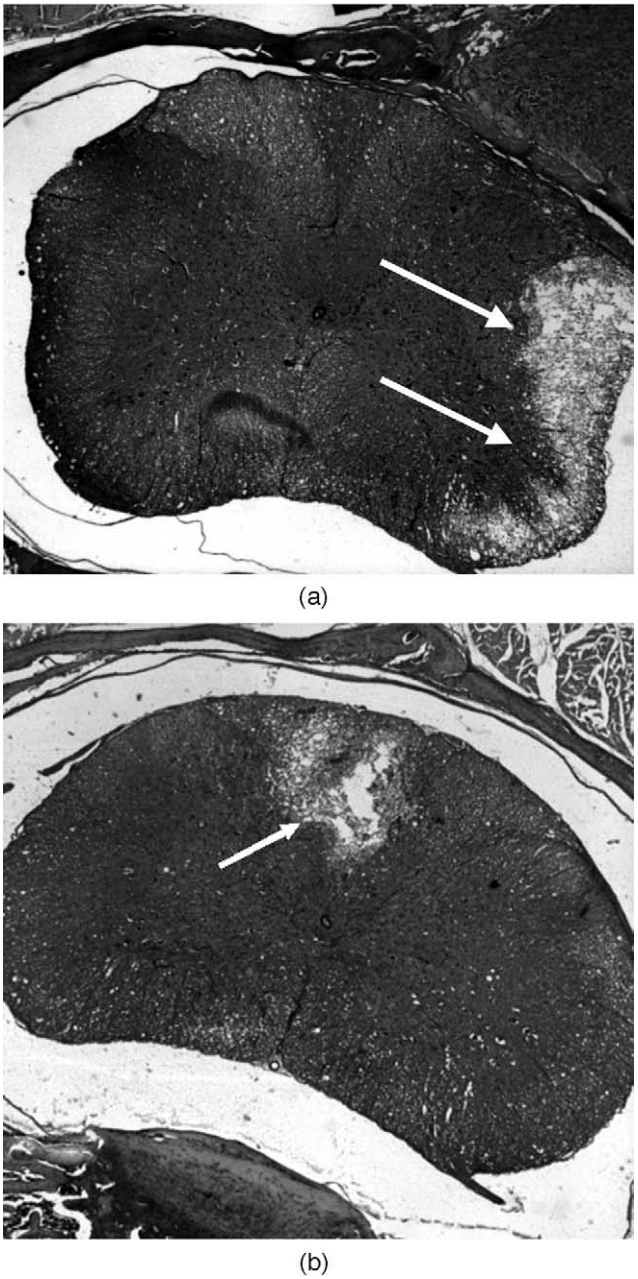

Fig. 5. Transverse sections of the rat cervical spinal cord at the level of the C4 (hematoxylin-eosin stained). Extensive white matter necrosis is seen in the left lateral column (white arrows) after grazing beam irradiation (a). After central beam irradiation, extensive white matter necrosis is observed in the dorsal column of the white matter (white arrow) without major lesions in the lateral columns or gray matter (b).

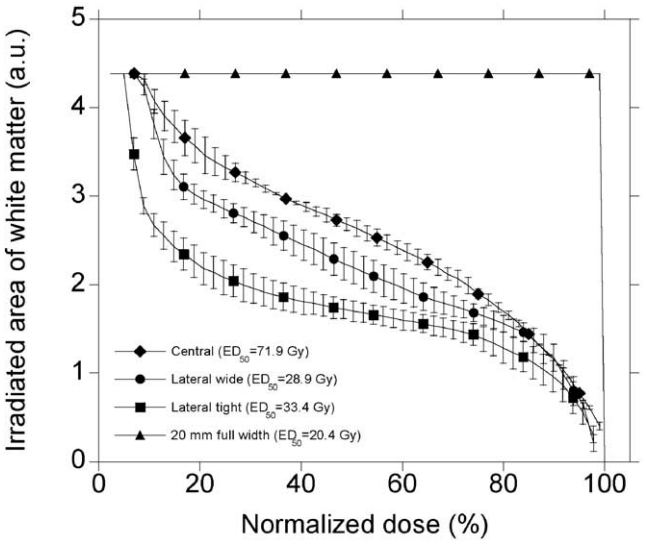

Fig. 6. Dose–area histogram for the lateral wide (black circles), lateral tight (black squares), and central beam (black diamonds) experiments compared with the 20-mm full-width irradiation (black triangles). The curves are normalized at the ED_{50} levels. The error bars indicate the combination of the mean positioning uncertainty of the 50% dose level and the movement uncertainty.

The latent periods varied from 62.5 days (± 2.8 days) to 98 days (Fig. 4).

Histologic examination of the spinal cord tissue of the paralyzed rats showed areas of white matter necrosis only in the middle part of the cord ($D_{max} \geq 60$ Gy) (Fig. 5b). The doses applied to the lateral parts of the white matter ranged from 10% to 50% of D_{max} (D_{max}: 20–80 Gy) and were not associated with morphologic changes. The gray matter and the peripheral nerve roots showed no morphologic changes, indicating that the paralysis was resulting from the white matter necrosis. In none of the rats with a follow-up period of up to 20 months were neurologic deficits observed. Spinal cord tissue from nonresponders showed no abnormalities in peripheral nerve roots or white or gray matter.

Dose–area histograms

The dose–area histograms normalized at the ED_{50} levels for the three present experiments and for the 20-mm full-width irradiation are plotted in Fig. 6. It can be seen that the area of irradiated white matter for the central beam experiment is larger at almost all dose levels compared with the lateral wide and tight curves.

DISCUSSION

With a high-precision proton beam, this study showed that the white matter in the left lateral half of the mature rat cervical spinal cord was more sensitive to radiation than the white matter in the middle part. This is expressed in a large shift to higher doses of the dose–response curve for the central beam compared with the grazing beams (Fig. 3), with a significantly higher radiosensitivity (ED_{50} values of 71.9 Gy compared with 28.9 and 33.4 Gy for the grazing beam experiments; Table 1). The shift for all dose–response curves was significantly different from that of the 20-mm full-irradiated single field (Fig. 3). The large difference between the radiosensitivity for the central beam and the grazing beam experiments is not simply a volume effect but is based on regional differences in radiosensitivity within the white matter. In case of a volume effect, it would be expected that the ED_{50} increased with decreasing irradiated volume. As can be observed in Fig. 6, the irradiated volume of white matter for the central beam is larger at almost all dose levels compared with the grazing beam experiments. Histologic examination of the paralyzed rats revealed that paralysis was due to white matter necrosis (Figs. 5a and 5b), and no abnormalities were observed in the gray matter even after a single dose of 80 Gy.

The difference in radiosensitivity between the gray matter and white matter is likely a result of anatomic and physiologic differences in different parts of the spinal cord. The vascular supply and density are different for the white matter and gray matter. Koyanagi *et al.* (15) showed that the sulcal arteries supply most of the gray matter and white matter in the ventral and lateral spinal cord. The posterior gray matter and white matter are fed from the posterior spinal arteries (15). The investigators observed in the gray matter a butterfly-shaped rich capillary network, whereas the anterior and lateral white columns were characterized by radially oriented vessels. The posterior column contains two large veins for drainage of the posterior columns, medial posterior gray matter, and posterior gray matter. Other parts of the cord are drained by the sulcal veins and radial veins (15). The arterial supply results in a centripetal and centrifugal blood flow pattern in the cord. In the white matter and in the dorsal half of the gray matter, the local blood flow is mainly provided by the centripetal system, whereas the ventral part of the gray matter derives its flow from the centrifugal system (16). Regionally, the vascular density is higher in the gray matter than in the white matter and higher in the ventral half of the gray matter than in the dorsal half (16). The ratio of vascular density and blood flow in gray matter to white matter is approximately 3:1 (16, 17). The blood flow in the white matter has a relatively homogeneous pattern, whereas the gray matter has a more variable blood flow with topography (16). Therefore, the regional difference of radiosensitivity within the white matter is not only the result of vascular damage because there is no regional difference in vascular density or blood flow within the white matter.

The endothelial cell is currently indicated as a major target in the pathogenesis of white matter necrosis, as observed after selective irradiation of blood vessels in rat spinal cord with ^{10}Boron agents (6). Acute vascular changes appear within 24 hours after irradiation and include increased endothelial swelling, vascular permeability and edema, lymphocyte adhesion and infiltration, and apoptosis (17–22). In a murine whole body irradiation model, Paris *et*

al. (19) observed that early endothelial apoptosis in the gastrointestinal (GI) tract was the primary lesion leading to stem cell dysfunction, resulting eventually in the GI syndrome (19). The GI syndrome was prevented by administering basic fibroblast growth factor (bFGF). It was shown that the endothelial cells and not the crypt cells were expressing FGF receptor transcripts. Similar modulating effects with growth factors were observed after irradiation of the rat spinal cord (23). Platelet-derived growth factor, insulin-like growth factor-1 (IGF-1), and vascular endothelial growth factor reduced the radiation myelopathy rates. Combining IGF-1 with bFGF showed a further decrease of the incidence of radiation myelopathy (23).

The role of OPCs in the pathogenesis of white matter necrosis is not clear. It is shown that the distribution of OPCs is nonuniform in the spinal cord. In the adult rat spinal cord, OPCs are located in the outer circumference of the cord, with no significant differences between dorsal, lateral, or ventral regions (24). The present experiments show that the lateral half of the white matter is more radiosensitive than the middle section of the white matter. Several studies showed that areas depleted of progenitors by irradiation repopulated slowly by OPCs from adjacent unirradiated areas (7–9). The higher radioresistance of the middle part of the white matter might be the result of migration of progenitor cells from the OPC regions in the lateral white matter of the cord. In the central beam experiment, this region received a dose $\leq$20% of D_{max} (range, 4–16 Gy). Hinks *et al.* (8) showed that depletion of OPCs in a rat spinal cord segment occurred after a single dose of 40 Gy. Because the migration distance of OPCs is limited to approximately 2 mm (9), the contribution of migration in a longitudinal direction from unirradiated adjacent areas is negligible. The migration of OPCs from both lateral parts to the middle part of the white matter is $<$2 mm and is not hampered by anatomic obstacles. However, in the grazing beam experiments, the migration of OPCs is only from one side (from the right lateral white matter to the contralateral irradiated white matter) and is partially hampered by the anterior median fissure and posterior median septum of the cord. The difference in radiosensitivity between the lateral wide (penumbra: 1.1 mm) and tight experiments (penumbra: 0.8 mm) is possibly the result of a relatively low dose (bath dose) to the right lateral half of the white matter, which affects the OPC population. The bath dose to this region ranged 4–8 Gy for the lateral wide and 2.4–3.6 Gy for the lateral tight. The higher bath dose in the lateral wide experiment possibly resulted in a smaller OPC population compared with the lateral tight experiment, which expressed itself in a slightly higher radiosensitivity due to a less efficient migratory capacity of the surviving OPCs (Table 1). A similar effect of different bath doses was reported in a previous study, in which inhomogeneous dose distributions were applied along the cord (4).

CONCLUSIONS

This study showed for the first time large differences in radiosensitivity within the rat cervical spinal cord. These observations show that the lateral white matter is more radiosensitive than the central part of the white matter, suggesting that white matter necrosis is not just due to vascular endothelial damage, assuming the capillaries in the white matter to be homogeneously distributed. The migration of progenitor cells is possibly involved in the restoration of radiation-induced white matter damage. The gray matter is highly resistant to radiation: no lesions were observed even after a single dose as high as 80 Gy. These results might be important for the estimation of normal tissue complication probabilities for high-precision radiation techniques.

REFERENCES

1. Bijl HP, Van Luijk P, Coppes RP, *et al.* Dose-volume effects in the rat cervical spinal cord after proton irradiation. *Int J Radiat Oncol Biol Phys* 2002;52:205–211.
2. Hopewell JW, Morris AD, Dixon-Brown A. The influence of field size on the late tolerance of the rat spinal cord to single doses of X rays. *Br J Radiol* 1987;60:1099–1108.
3. Van der Kogel AJ. Dose-volume effects in the spinal cord. *Radiother Oncol* 1993;29:105–109.
4. Bijl HP, Van Luijk P, Coppes RP, *et al.* Unexpected changes of rat cervical spinal cord tolerance caused by inhomogeneous dose distributions. *Int J Radiat Oncol Biol Phys* 2003;57:274–281.
5. Nieder C, Ataman F, Price RE, *et al.* Radiation myelopathy: New perspective on an old problem. *Radiat Oncol Invest* 1999;7:193–203.
6. Morris GM, Coderre JA, Whitehouse EM, *et al.* Boron neutron capture therapy: A guide to the understanding of the pathogenesis of late radiation damage to the rat spinal cord. *Int J Radiat Oncol Biol Phys* 1994;28:1107–1112.
7. Chari DM, Blakemore WF. Efficient recolonisation of progenitor-depleted areas of the CNS by adult oligodendrocyte progenitor cells. *Glia* 2002;37:307–313.
8. Hinks GL, Chari DM, O'Leary MT, *et al.* Depletion of endogenous oligodendrocyte progenitors rather than increased availability of survival factors is a likely explanation for enhanced survival of transplanted oligodendrocyte progenitors in X-irradiated compared to normal CNS. *Neuropath App Neurobiol* 2001;27:59–67.
9. Franklin RJ, Gilson JM, Blakemore WF. Local recruitment of remyelinating cells in the repair of demyelination in the central nervous system. *J Neurosci Res* 1997;50:337–344.
10. Van Luijk P, Bijl HP, Van der Kogel AJ, *et al.* Techniques for precision irradiation of the lateral half of the rat cervical spinal cord using 150 MeV protons. *Phys Med Biol* 2001;46:2857–2871.
11. Boon SA, Van Luijk P, Schippers JM, *et al.* Fast 2D phantom dosimetry for scanning proton beams. *Med Phys* 1998;25:464–475.
12. Van Luijk P, Van't Veld AA, Zelle HD, *et al.* Collimator scatter and 2D dosimetry in small proton beams. *Phys Med Biol* 2001;46:653–670.
13. Van der Kogel AJ. Late effects of radiation on the spinal cord. Rijswijk: Radiobiological Institute TNO. 1979.
14. Van der Kogel AJ, Sissingh HA, Zoetelief J. Effect of X-rays and neutrons on repair and regeneration in the rat spinal cord. *Int J Radiat Oncol Biol Phys* 1982;8:2095–2097.
15. Koyanagi I, Tator CH, Lea PJ. Three-dimensional analysis of

the vascular system in the rat spinal cord with scanning electron microscopy of vascular corrosion casts. Part 1: normal spinal cord. *Neurosurgery* 1993;33:277–284.
16. Hayashi N, Green BA, Gonzalez-Carvajal M*, et al.* Local blood flow, oxygen tension, and oxygen consumption in the rat spinal cord. Part 1: Oxygen metabolism and neuronal function. *J Neurosurg* 1983;58:516–525.
17. Stewart PA, Vinters HV, Wong CS. Blood–spinal cord barrier function and morphometry after single doses of X-rays in rat spinal cord. *Int J Radiat Oncol Biol Phys* 1995;32:703–711.
18. Li YQ, Ballinger JR, Nordal RA*, et al.* Hypoxia in radiation-induced blood-spinal cord barrier breakdown. *Cancer Res* 2001;61:3348–3354.
19. Paris F, Fuks Z, Kang A*, et al.* Endothelial apoptosis as the primary lesion initiating intestinal radiation damage in mice. *Science* 2001;293:293–297.
20. Peña LA, Fuks Z, Kolesnick RN. Radiation-induced apoptosis of endothelial cells in the murine central nervous system: Protection by fibroblast growth factor and sphingomyelinase deficiency. *Cancer Res* 2000;60:321–327.
21. Tsao MN, Li YQ, Lu G*, et al.* Upregulation of vascular endothelial growth factor is associated with radiation-induced blood-spinal cord barrier breakdown. *J Neuropathol Exp Neurol* 1999;58:1051–1060.
22. Siegel T, Pfeffer MR. Radiation-induced changes in the profile of spinal cord serotonin, prostaglandin synthesis, and vascular permeability. *Int J Radiat Oncol Biol Phys* 1995;31:57–64.
23. Nieder C, Price RE, Andratschke N*, et al.* Biological prevention of radiation-induced late central nervous system injury by treatment with growth factors. In: Dörr W, editor. Growth factors in the pathogenesis of radiation effects in normal tissues. 1st ed. Munich: Urban and Vogel; 2001. p. 58–61.
24. Horner PJ, Power AE, Kempermann G*, et al.* Proliferation and differentiation of progenitor cells throughout the intact adult rat spinal cord. *J Neurosci* 2000;20:2218–2228.